SKB rapport R-97-19

December 1997

System and safety studies of accelerator driven transmutation systems

Annual report 1997

Jan Wallenius, Johan Carlsson, Waclaw Gudowski

Department of Nuclear & Reactor Physics,
Royal Institute of Technology, Stockholm

SKB, Box 5864, 102 40 Stockholm
Telefon 08-665 28 00 • Telefax 08-661 57 19 • Telex 13108 S

ISSN 1402-3091
SKB Rapport R-97-19

SYSTEM AND SAFETY STUDIES OF ACCELERATOR DRIVEN TRANSMUTATION SYSTEMS

ANNUAL REPORT 1997

Jan Wallenius, Johan Carlsson, Waclaw Gudowski

Department of Nuclear & Reactor Physics,
Royal Institute of Technology, Stockholm, Sweden

December 1997

System and safety studies of accelerator driven transmutation systems

Annual report 1997

Jan Wallenius, Johan Carlsson and Waclaw Gudowski

Department of Nuclear & Reactor Physics

Royal Institute of Technology

TABLE OF CONTENTS

INTRODUCTION

In November 1996, SKB started financing of the project "System and safety studies of accelerator driven transmutation systems and development of a spallation target". The aim of the project was stated as:

1) Development of a complete code for simulation of transmutation processes in an accelerator driven system. Application of the code for analysis of neutron flux, transmutation rates, reactivity changes, toxicity and radiation damages in the transmutation core.

2) Build up of competence regarding issues related to spallation targets, development of research activities regarding relevant material issues. Performing of basic experiments in order to investigate the adequacy of using the spallation target as a neutron source for a transmutation system, and participation in the planning and implementation of an international demonstration-experiment.

In the present report, activities within the framework of the project performed at the department of Nuclear & Reactor Physics at the Royal Institute of Technology during 1997, are accounted for.

SIMULATION OF PARTICLE TRANSPORT

This part of the project was performed by research associate Jan Wallenius together with PhD student Kamil Tucek and guest scientist Aleksander Polanski. Results from Diploma theses made at the department also appeared to be useful. Research associate Adam Soltan participated in the processing of evaluated nuclear data files for use in the simulations.

Spallation

Aleksander Polanski from the Soltan-institute in Warsaw visited the department twice during 1997 for work on Monte-Carlo simulations of the spallation process. The process can shortly be described as nuclear reactions that take place when a lighter nucleus (in transmutation studies, mainly protons are discussed), accelerated to energies of the order of 1 GeV, hits a heavier nucleus. Initially, a few nucleons with relatively high energy are ejected. Then, the excited target nucleus relaxes by evaporating several additional nucleons. The higher the projectile energy, the larger number of nucleons are emitted. The main part of the emitted nucleons are neutrons, which can be used as a neutron source for a sub-critical transmutation core.

Codes simulating the spallation process generally rely on theoretical predictions of nucleon-nucleus cross sections that are adjusted to fit existing experimental data, which for some energy ranges can be scarce. The projectile is usually transported inside the target nucleus using Monte-Carlo methods, yielding statistical distributions of emitted nucleons and nuclei.

Polanski did previously participate in the development of a Russian code (DUBNA-CE) for simulation of this process, which in comparison with experimental results for neutron yields and spallation product distributions in thin targets, generally exhibits

better predictive capability than other existing codes [1]. However, during the year it appeared that in order to make a sufficiently good simulation of neutron production in larger targets, a better model for neutron transport *in-between* nuclear collisions than provided by the Russian code, was needed. Polanski therefore recommended to use a code with good transport capabilities as a frame for the code development, and to that code add improved theoretical calculations of nuclear reaction cross sections in high energy nucleon-nucleus collisions.

An investigation of FLUKA [2] made by Johan Carlsson [3] showed that FLUKA in principle could be used for calculation of neutron fluxes, spallation product yields and toxicity in extended targets. Carlo Rubbia's Emerging Energy Technology group also uses FLUKA for simulation of high energy processes in their studies of accelerator driven systems. Nevertheless, Alberto Talamo's diploma thesis showed that FLUKA results for spallation product yield were rather suspicious [4]. Further, it turned out that the present author of FLUKA, Alfredo Ferrari, did not agree on sharing the source code with other scientists. Hence attention was transferred towards LAHET (Los Alamos High Energy Transport code) [5], which features a complex treatment of particle transport in arbitrary materials, including an advanced geometry setup developed for the low energy transport code MCNP (see following section). The drawbacks of LAHET are, as previously mentioned, that the predicted yield of spallation products in many cases does not agree with experimentally measured yields. Further, the angular distribution of emitted particles seems not to agree with experimental distributions measured for thin targets.

During the fall of 1997, cooperation with the author of LAHET, Richard Prael, was initiated, leading to an agreement where Polanski is writing subroutines for inclusion of improved theoretical cross sections into the upcoming version (3) of LAHET. The result of this cooperation is assumed to be a significant improvement in LAHET predictions of spallation product yields, which consequently gives a better basis for a correct prediction of induced target radiotoxicity. LAHET version 3 thus is adopted as the choice of simulation code for high energy scattering (E 150 MeV) in the integrated code package that the present project is expected to produce.

Neutronics

During 1997, Jan Wallenius and Kamil Tucek used MCNP (Monte Carlo N-Particle transport code) [6] for calculations of neutron spectra and neutron economy in different types of accelerator driven systems. During spring the activity was concentrated to participating in IAEA:s Coordinated Research Program (CRP) on neutronics of accelerator driven systems. In this program calculations of neutron multiplication, neutron spectrum, power density and burnup for a sub-critical Th232/U233 lead cooled core with oxide fuel were performed by research groups from ten different laboratories [7]. This system is very similar to the "Energy Amplifier" concept put forward by Carlo Rubbia. Continuous energy cross sections for neutron scattering were adopted from European and American evaluated nuclear data files and processed to take into account Doppler broadening effects at different temperatures (300K, 600K, 900K and 1200K). Cross sections of 30 actinides and 180 fission products were taken into account in the Monte Carlo simulation of neutron spectra, neutron multiplication and power density at each time step of the burnup.

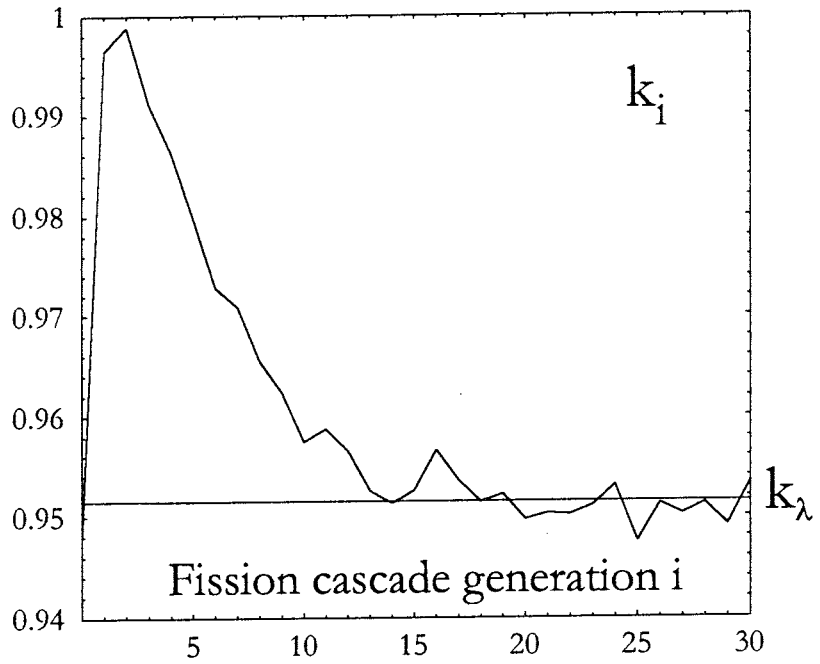

Figure 1: Neutron multiplication as function of fission generation in a sub-critical core using a spallation target as neutron source. Generation # zero denotes spallation neutrons. A simplified model of a sodium cooled core with metallic U238/Pu239 fuel was assumed. Asymptotically the multiplication coefficient k relaxes to the value of 0.951, whilst the neutron flux is in transient mode with k 0.96 until fission number ten of the cascade. The effective neutron multiplication thus is ~ 30 % larger than what naively may be assumed from the value of k_{eff} (defined as the eigenvalue to the neutron transport equation).

MCNP in criticality mode was also used to calculate effective neutron multiplication for each individual fission cascade generation. As shown in figure 1, the neutron flux is in transient mode well beyond the 10^{th} fission generation also for sodium cooled plutonium breeding sub-critical cores, which means that fundamental mode analysis partially looses relevance for neutronics and safety analysis of sub-critical systems

Since sub-critical cores with homogeneous fuel composition exhibit much larger gradients in neutron flux and concomitant power density than analog critical cores do (see figure 2), the total power of the system is limited by maximal allowed power density (cooling capacity) and radiation damages in central parts of the core. As power is proportional to the number of fissioning actinide nuclei, one has an inferior transmutation efficiency in outer parts of the core, in comparison with critical configurations. This can be compensated for by use of an inhomogeneous fuel composition, with an increased fraction of thermally fissionable isotopes in outer core fuel elements. Such power density flattening strategies are used in modern light water reactors, but can be made even more flexible in a sub-critical system, which does not need not rely on delayed neutrons for safety in case of accidental criticality insertions. One might consider fuel elements with pure transuranic composition in outer core parts, with an increased fraction of U238 or fission products in inner regions.

With several years of experience using the continuous energy MCNP transport code, we conclude that the code is an accurate tool for simulating neutronics of sub-critical cores, which excludes errors in calculation due to the calculation method itself. This is

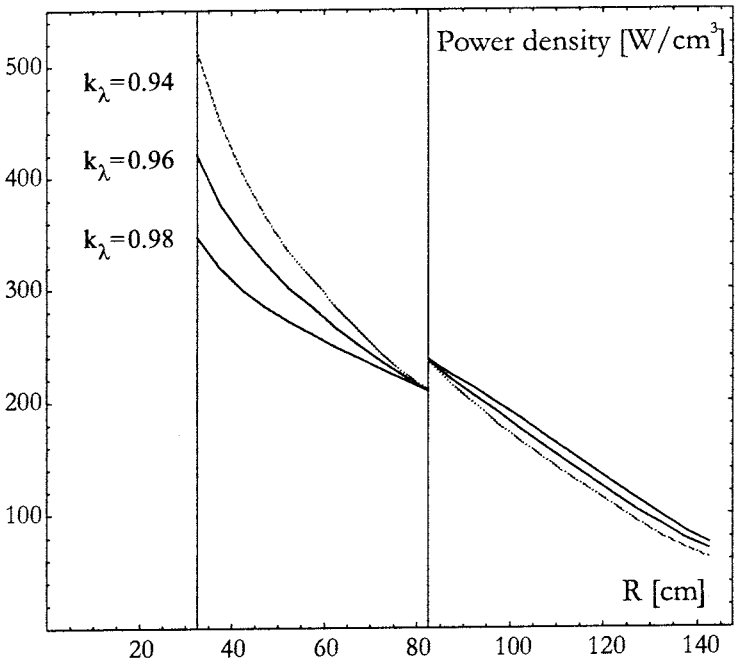

Figure 2: Power density in a sub-critical Th232/U233 oxide fuel core with fast spectrum, as function of radius and eigenvalue k_λ to the neutron transport equation. A total power of 1500 MWth was assumed. Even though liquid metal coolants allow for power densities around 300 W/cm³ in oxide fuel cores, one finds that this limit is exceeded in the vicinity of the spallation target. This problem can be resolved by introducing an inhomogeneous fuel element composition.

in the authors' opinion an advantage over multi-group codes, where results might be sensitive to bad group structuring and self-shielding corrections in an unpredictable way. Continuous energy Monte-Carlo codes and deterministic multigroup codes both suffer from the same potential errors in underlying cross section evaluation data, however.

Burnup

Simulation of transmutation processes in sub-critical systems over extended periods of time, so called burnup, was made using the ORIGEN2 code (Oak Ridge Isotope GENeration and depletion code) [9]. The code uses effective one-group cross sections for transmutation reactions like fission, neutron capture and neutron knockout, that have to be calculated with an external neutronics code for each specific system. The department calculated these one-group cross sections with MCNP for all actinides and those of the fission products for which transport cross sections existed in the European evaluated nuclear data library (~ 180), in each separate MCNP-cell. Specifying an average power of the cell subject to burnup, ORIGEN2 converts this power to an average neutron flux, which is used in conjunction with the one-group cross section library for calculating transmutation rates. The transmutation process, i.e. the change in isotopic composition over time is then calculated by solving the Bateman equations, taking into account natural decay of all nuclides. ORIGEN2 provides "default" cross sections for a range of reactor types for a total of 1400 nuclides, which are used in the burnup for those isotopes that we did not calculate cross sections using MCNP.

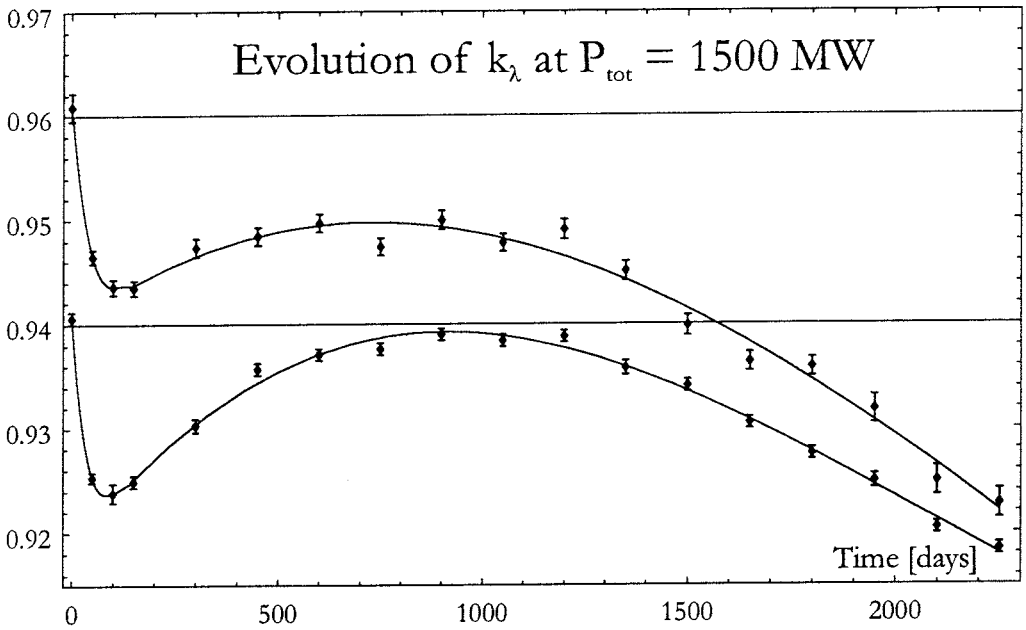

Figure 3: Evolution over time of the eigenvalue k_λ in a lead cooled sub-critical Th232/U233 core, at a constant power of 1500 MWth. Point data with error bars are eigenvalues calculated with MCNP in criticality mode, for fuel compositions predicted with the MCNP/ORIGEN2 package.

Simulation of burnup for the IAEA CRP mentioned above was made using the MCNP/ORIGEN2 package. Results for the time development of the eigenvalue k_λ to the neutron transport equation at a constant power of 1500 MWth in the lead cooled core, are displayed in figure 3 for two initial values of k_λ . A higher initial k_λ gives, according to these results, a larger reactivity loss over the burnup cycle.

During the fall of 1997 the MCNP/ORIGEN2 coupling was automatized step by step, leading to the completition of a BURN[r] package where no manual editing of files are needed to perform burnup calculations in up to 100 core regions in-between consecutive MCNP runs for adjusting one-group cross sections and individual cell fluxes.

During this work several drawbacks of ORIGEN2 burnup treatment were realized. First, mechanisms for controlling spectrum changes during burnup calculations are missing, which may lead to problems when isotopes with high absorption cross sections appear in the fuel. Second, the fission product yield as function of incident neutron energy is treated in an over simplified manner. Experimental data for the fission product yields exist virtually only for two single neutron energies, which ORIGEN2 uses in accordance with a user specification of either a "thermal" or a "fast" spectrum. In addition, ORIGEN2 gives explicit fission product yields for a maximum of eight actinides.

Hence, an initiative was taken to create an internal burnup module to MCNP, which is anticipated to manage handling of spectrum changes during burnup consistently, and further will be using theoretical models for predicting the incident neutron energy dependence of fission product yields. Work on this module was started in November 1997 in cooperation with Jerzy Cetnar from the University of Cracow.

PROJECT MILESTONES

Milestone number one, for part one of the project was defined as "Choice of relevant computer codes as frames for developing an integrated code package, and definition of necessary improvements". In the present report, this choice is clearly presented together with the improvements to the codes deemed necessary to make. In conclusion:

- LAHET version 3 with new subroutines for improved predictive capability of spallation product yield, will be used for simulation of high energy particle transport.
- MCNP will be used for neutronics simulations.
- A new program for calculation of burnup, intended for integration with MCNP, needs to be developed.

WORK PLAN FOR 1998

Integration of LAHET version 3 and MCNP will be done in cooperation with the APT group of Los Alamos National Laboratory, which has initiated a similar code integration project for simulation of Accelerator based Production of Tritium systems. The integration will make possible the use of evaluated nuclear scattering data also for particle energies in the energy region 20-150 MeV, for a number of isotopes. The agreement with the APT group consists of our group writing a complete burnup module, and defining unified formats for fission product treatment. In return, we will then be given access to MCNPX, in which LAHET version 3 will function as a subroutine to an extended MCNP being capable of transporting arbitrary particles at arbitrary energies. The transition from use of calculated cross sections at particle energies above 150 MeV to library cross sections at lower energies will be implemented in a flexible way, allowing for different treatment for different isotopes, depending on availability of experimental data. Hence, the activities of the department during 1998 can be concentrated to work on subroutines for LAHET version 3 in cooperation with the Soltan institute in Warsaw, and completition of the burnup module, in cooperation with the University of Cracow.

INVESTIGATION OF SPALLATION TARGET PROPERTIES

Demonstration experiment

ISTC project number 559 was being under preparation during 1997. We defined and agreed on a work plan for the Institute of Physics and Power Engineering (IPPE), which in the framework of this project will design and construct a liquid lead/bismuth spallation target rated for 1 MW proton beam power. This work plan was subsequently approved by the ISTC partners (Sweden, EU and USA). A list of equipment necessary to acquire beside what is guaranteed by ISTC was prepared.

The project was de jure (and de facto) launched on January 1st 1998.

Liquid lead/bismuth loop experiment

In cooperation with Los Alamos National Laboratory, experimental activity concerning lead/bismuth as a core coolant was initiated. Preparations for a lead/bismuth loop experiment on location in Stockholm started.

Workshop on accelerator driven systems

An international workshop on the physics of accelerator driven systems for nuclear transmutation and clean energy generation was arranged by the department in cooperation with LANL. The conference was held in Trento, Italy September, from the 29th of September to the 3rd of October. The number of participants were 75, of which 25 were Italians, 10 from CERN, 6 Russians, 5 French, 5 Americans (LANL), 4 Swedish, 3 Spanish and 3 Germans.

Among the presentations was a talk by IPPE scientist Y. Orlov on lead/bismuth technology, concluding that a proper oxygen concentration in Pb/Bi prevents corrosion. If it is too high it can lead to Pb or Bi oxidation, while it must still be high enough to form Fe_3O_4 and Cr_2O_3 oxide crusts. The ideal oxygen concentration depends on the temperature, therefore one must avoid too big temperature differences.

Thermohydraulic calculations

Johan Carlsson spent the fall of 1997 in ISPRA, Italy for studying and performing thermohydraulics calculations for liquid lead and lead/bismuth used as spallation targets and fast spectrum core coolants.

After arriving to JRC Ispra, Johan made a literature survey, starting with Prof. Rubbia's reports on Accelerator Driven Systems [10].He also studied reports on the American research by General Electric, GE, on heavy liquid metal cooled systems (SAFR and PRISM), which were done during the 80's [11,12,13]. Their similarities to Prof. Rubbia's proposal made them important and relevant. For example, Rubbia's concept as well as PRISM and SAFR were designed to have the ability to remove decay heat after a scram exclusively by air. This can be done by natural convection around the reactor vessel. One could say that Rubbia's proposal is a development of this, but he uses double reactor vessels with isolating gas in between to reduce the parasitic losses during regular operation. When the temperature in the vessel increases considerably this isolating space is filled by lead, this is because lead expands with increasing temperature and thereby increases the lead level, after a while it runs over the edge of

the reactor vessel and thereby fills the gap. Calculations on the American version were also done by an independent research team (Brookhaven National Laboratory, BNL) which depicted that the decay heat removal could be accomplished and that it was as good as fail proof (even at an earthquake) since it was not dependent on human nor electrical/mechanical reliability.

PRISM had an oblong shape, to enhance natural circulation, which resembles of the Rubbia version. It is also hang up on similar shock absorbers which can handle catastrophes like earthquakes. There are of course differences, the biggest is that PRISM not has an accelerator nor a sub-critical core. To add, the PRISM design are of nine reactor collected in one block where each one produced about 400 MWth. One of the purposes with smaller reactors was to avoid a positive void coefficient in the coolant.

Studies on the safety systems of BWR and PWR, which are of interest since most of the safety functions are similar in ADS as well.

Flow3D, results

The intention of an experiment that is prpoposed to be situated at JRC Ispra is to prove that cooling of the core can be done by enhanced natural circulation, the enhanced circulation would be accomplished by inserting Argon bubbles above the core. They also want to check if decay heat can be removed by exclusively air by natural convection outside the vessel.

Some calculations done with Flow3D are going to be used for an experiment which might be situated at JRC. They are aimed to design the reactor vessel with emphasize on avoiding swirls and that it should be possible to remove decay heat by solely air. See figure 4.

Examples of parameters to vary is the relative dimension between the up-comer and the down-comer, Johan's calculations showed that a relationship of 3:1 instead of 4:1 was better due to less swirls in the top region of the vessel. One more example is the height of the wall between the up-comer and down-comer above the bottom of the reactor vessel should end, if it ends too close to the bottom swirls will develop. A last example is the shape of the bottom of the vessel, we found that an elliptical shape instead of spherical decreased the swirls.

Regarding the cooling of the vessel by air calculations with fins and increased surface roughnes and, dimension of channels were made. Unfortunately are these calculations not satisfactory since radiation heat transfer cannot be handled, and the Boussinesq approximation is not applicable.

At LANL, Los Alamos National Laboratory, a full scale experiment on a target with an accelerator will start 1999. The target is manufactured in Obninsk, Russia. Two Russian designs, were investigated, see figures 5 and 6. The coolant is Pb/Bi, flow rate 14 m^3/h, and at inlet the temperature is 220°C. The proton beam is of 800 MeV and 1250 mA.

In the asymmetrical target the gravity is acting in the negative x-direction and the beam is inserted horisontally. The maximum temperature becomes circa 520°C and is located behind the separating wall because the flow is not as developed there. The fact that the most elevated temperature is close to the separating wall is not good in the view point of corrosion control.

In the symmetrical target with gravity acting in negative z-direction and the beam inserted from the top of the picture. The maximum temperature is here about 560°C. If the gravity acts in the opposite direction, positive z-direction, the maximum temperature is nearby 510°C. The difference is due to that the buoyancy forces is working opposite and in the direction of the heated flow respectively.

Russian scientists have performed two dimensional calculations which my results will be compared with eventually.

Flow3D, problems occurred

The reason for Flow3D was chosen was that it could handle freezing. Since the present work was supposed to handle freezing problems in a lead cooled Accelerator Driven System, this seemed to be the appropriate choice.

After weeks of usage and learning, the conclusion that Flow3D has limitations which could not be compensated in a reliable way for the present problem was made. For instance, Flow3D can only treat two fluids at the same time (we will need at least three), of which only one can be compressible.

If one chooses to have two incompressible fluids in natural convection problems the Boussinesq approximation are not suitable for gases which are heated more than a few degrees or travel a height more than a couple of meters. Since one wans to remove the decay heat by natural convection of outside of the vessel where the air was heated about 150-200°C this was not a possible option.

Another problem is the lack of handling radiation heat transfer. In Rubbia's concept there are two vessels, the reactor vessel and outside of this the containment vessel. In between these vessels there will be an inert gas, here the radiation heat transfer is important and cannot be neglected. Flow3D can remove radiation from a surface but it is not transferred anywhere, it disappears.

Flow3D uses a structured mesh (orthogonal or cylindrical), this causes problems if small details are needed. This is because neighbouring cells should not be 30 % bigger or smaller due to stability considerations. Small details influence therefore the whole mesh. Star-CD, for instance, has an unstructured mesh where such limitations are not as severe.

Later at the Trento conference it looked like Pb/Bi would be chosen as coolant instead of Pb since the experience with that technology are larger. Russians has used Pb/Bi as coolant in their submarines for totally 70 reactor years. Therefore Pb/Bi will probably be the choice in the first versions of the Energy Amplifier. Thereby, the reason for choosing Flow3D disappeared, because Pb/Bi has a freezing point which is significantly lower than Pb, freezing of the coolant will probably never appear.

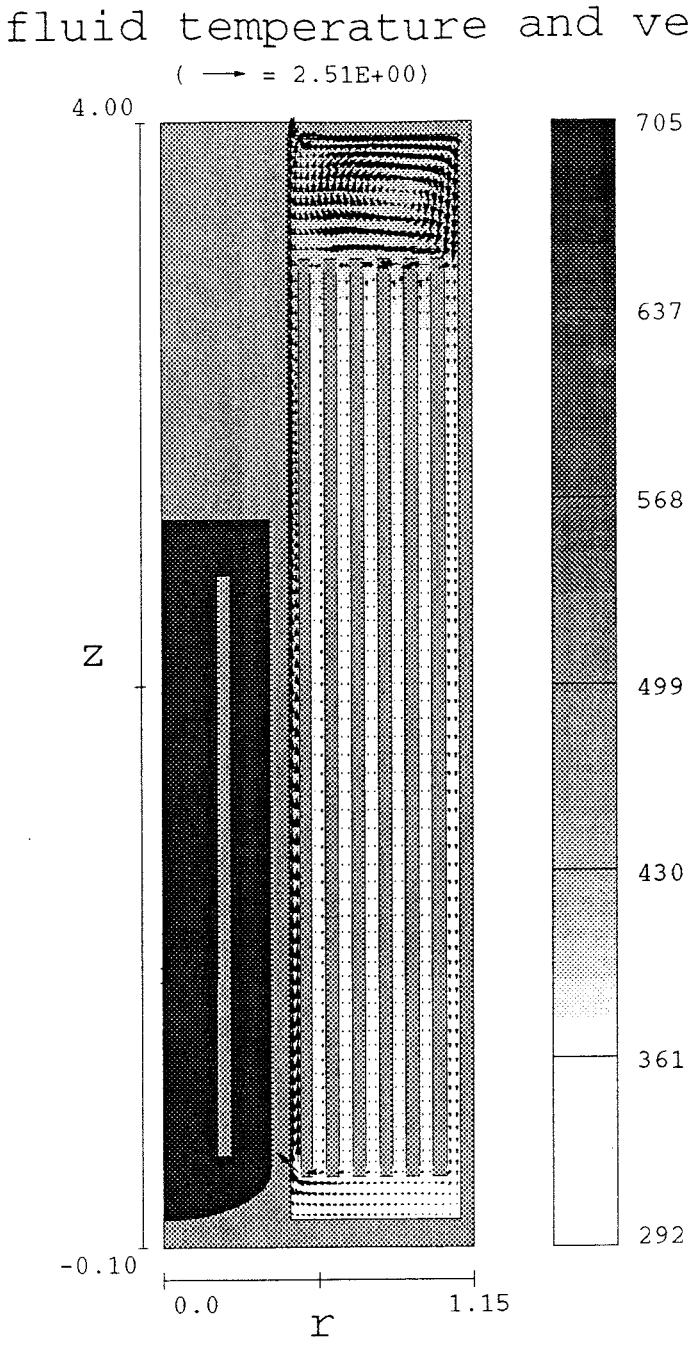

Figure 4: Flow 3D simulations of thermo hydraulics in a lead/bismuth vessel experiment.

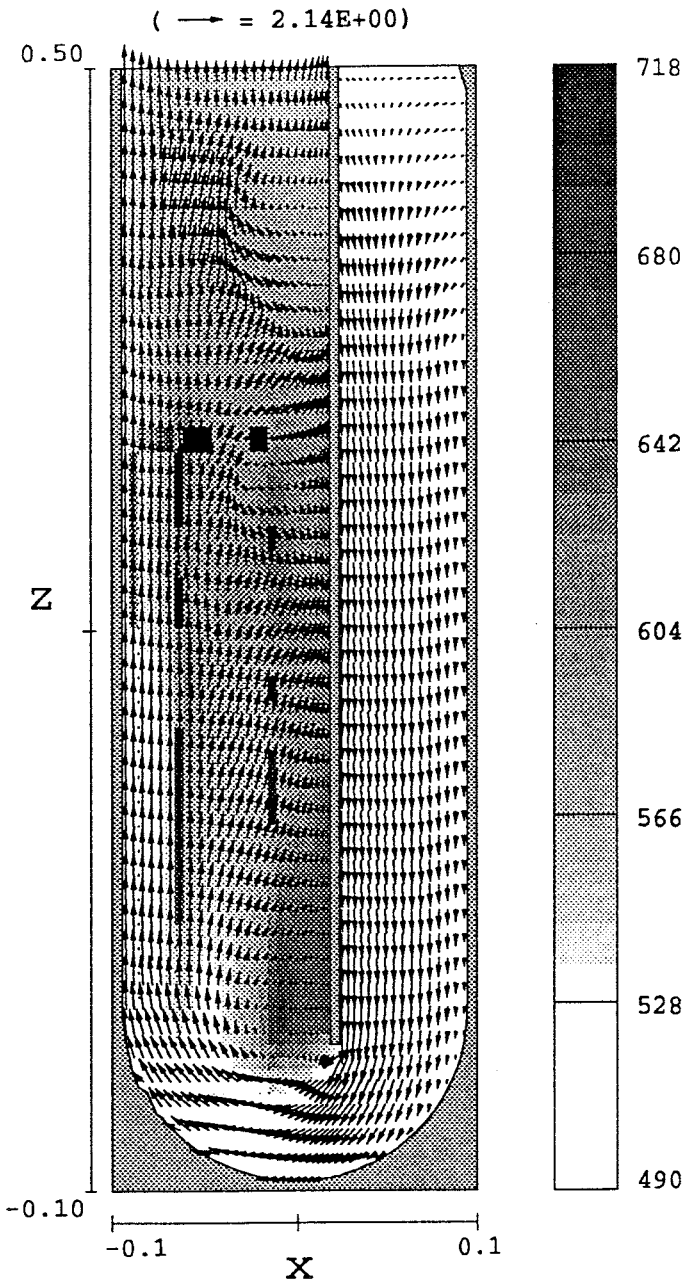

Figure 5: Flow 3D simulations of mass flow and temperature distribution in the asymmetric version of the russian liquid lead/bismuth spallation target.

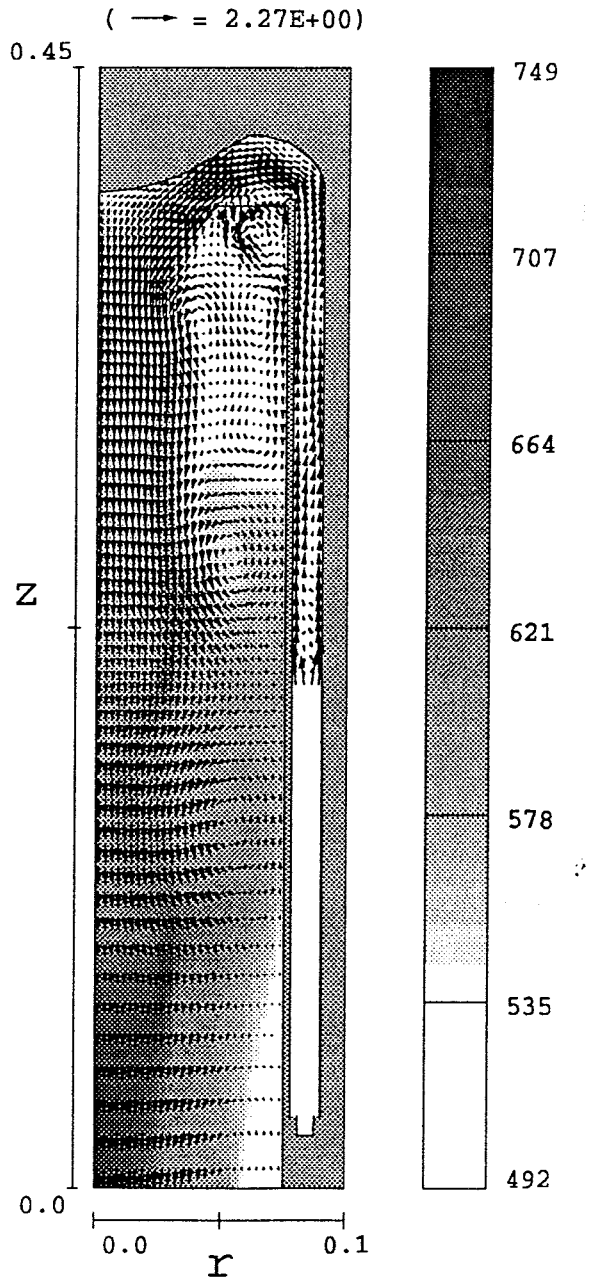

Figure 6: Flow 3D simulations of mass flow and temperature distribution in the symmetric version of the russian liquid lead/bismuth spallation target.

REFERENCES

[1] International codes and model intercomparison for intermediate energy activation yields. R. Michel and P. Nagel, editors, NEA P&T # 14 (1998).

[2] Alberto Fasso, Alberto Ferrari, Paola Sala and Johannes Ranft, FLUKA96 - manual, INFN (1996)

[3] Johan Carlsson, Optimization of the neutron production in a spallation target with FLUKA. M. Sc. Thesis, Department of Neutron and Reactor Physics, KTH (1996).

[4] Alberto Talamo, Studio della sorgente neutronica di spallazione per un sistema moltiplicante sottocritico. M.Sc thesis, Department of Energetics, Polytechnico di Torino, and Department of Nuclear and Reactor Physics, KTH (1997).

[5] Richard Prael and Henry Lichtenstein, User Guide to the LAHET code system, Los Alamos National Laboratory (1989)

[6] MCNP - A general Monte Carlo N-Particle transport code, version 4B, J.F.Briesmeister, editor, LA-12625-M, Los Alamos National Laboratory (1997).

[7] K. Tucek, J. Wallenius, W. Gudowski and A. Soltan, IAEA Accelerator Driven System Neutronic Benchmark. Proceedings of a Technical committee meeting on feasibility and motivation for hybrid systems in Madrid, 1997. IAEA (to be published).

[8] J. Wallenius, Transmutation of 137Cs and 129I using a muon catalyzed fusion neutron source, Fusion Technology (to be published).

[9] A. Croff, Nuclear Technology **62**, p. 335 (1983).

[10] C. Rubbia et al. Cern group conceptual design of a fast neutron operated high power energy amplifier. In Accelerator driven systems: Energy generation and transmutation of nuclear waste, editor W. Gudowski. IAEA-TECDOC-985, page 187. IAEA (1997)

[11] Preapplication Safety Evalution Report for the Sodium Advanced Fast Reactor (SAFR) Liquid-Metal Reactor, NUREG-1369, (1991).

[12] Evaluations of 1990 PRISM Design Revisons, NUREG/CR-5815 and BNL-NUREG-52311, (1992).

[13] Draft Preapplication Safety Evaluation Report for Power Reactor Inherently Safe Module Liquid Metal Reactor, NUREG 1368, (1989).

ATTACHMENTS

[1] K. Tucek, J. Wallenius, Waclaw Gudowski and Adam Soltan, IAEA Accelerator DrivenSystem Neutronic Benchmark. Proceedings of a Technical committee meeting on feasibility and motivation for hybrid systems in Madrid, 1997. IAEA (to be published).

[2] J. Wallenius, Transmutation of 137Cs and 129I using a muon catalyzed fusion neutron source, Fusion Technology (to be published).

IAEA Accelerator Driven System Neutronic Benchmark

Kamil Tucek, Jan Wallenius, Waclaw Gudowski and Adam Soltan
Department of Nuclear and Reactor Physics
Royal Institute of Technology, 100 44 Stockholm, Sweden.

ABSTRACT

Reactivity and burn-up simulations have been done for the first stage of the IAEA Co-ordinated Research Program on Accelerator Driven Systems. Neutron multiplication and flux distributions were calculated using the MCNP Monte-Carlo code. Multiplication eigenvalues to the neutron transport equation were obtained by running MCNP in the KCODE mode. Our investigation shows that the space-time dependent distribution of fission events features a *pronounced* generation dependence, which is an inherent property of sub-critical systems having separated neutron source and core/blanket regions. The power peaking in the vicinity of the external neutron source is enhanced by slowing down of fission neutrons in the spallation target. Thus the behaviour of the system is not well described by global parameters like eigenvalue, eigenflux or source importance. It is suggested that physically more relevant entities like effective multiplication constants and generation-dependent fission distributions should be used to characterize the system.

1) INTRODUCTION

In order to improve neutron economy and safety margins in reactors designed for transmutation of spent nuclear fuel, and/or nuclear fuel breeding purposes, inherent sub-criticality of the reactor core is introduced in combination with an external neutron source provided by proton induced spallation [1]. Since the effective neutron multiplication in sub-critical systems is very sensitive to the changes in fuel composition naturally appearing during burn-up, the proton current provided by the accelerator must be fairly flexible. Accurate modelling of the burn-up behaviour thus becomes essential for design and safety analysis of sub-critical systems. In order to investigate and validate scientific expectations, IAEA launched the Co-ordinated Research Program (CRP) on Accelerator Driven Systems (ADS). As a part of this programme, the ADS Benchmark Problem was issued. The purpose of the benchmark is to assess system performances like neutronic characteristics, transmutation potential etc., in order to achieve consensus on calculation methods and associated nuclear data. The benchmark problem is divided into several phases (stages). Stage one, objective of the present paper, is focused on uncertainties in calculated neutronic characteristics of a simple model thorium breeder, mainly the verification of a reactivity swing in the burn-up at different levels of sub-criticality. In the following section we discuss the theoretical framework of ADS analysis, before going into computational details of neutron transport and burn-up. In section four we display eigenvalues, effective multiplication coefficients, void effects, power distributions and burn-up behaviour for different enrichments of U233 and finally we discuss the implications of our results in section five.

2) THEORY

Many standard codes for simulating reactor behaviour are based on deterministic solutions to the neutron transport equation. Such codes utilize expansions over eigenmodes in order to model the deviations from the "persisting mode" in the neutron flux arising from sub-

criticality and the inhomogenity introduced by the spallation target. From the mathematical viewpoint, this is a fully valid approach. Neutron fluxes and power distributions obtained are generally in good agreement with results from Monte Carlo simulations, where the physical behaviour of the system is modelled by sampling particle trajectories. However, since the physical relevance of an eigenmode is partly lost in a sub-critical system, both terminology as well as global parameters of the deterministic approach become somewhat inadequate. It should thus be useful to apply a different set of parameters in the analysis of neutronic characteristics of such systems. For critical reactors, the fuel composition yielding the algebraically largest multiplication eigenvalue $k_\lambda = 1$ of the neutron transport equation

$$(\Omega \cdot \nabla + \Sigma_t)\phi = Q_s + \frac{1}{k_\lambda} Q_f \qquad (1)$$

where Σ_t is the total macroscopic cross section and Q_s and Q_f are the scattering and fission source terms, coincides with the transition from finite to infinite neutron multiplication. Therefore, it became customary to identify k_λ with the effective neutron multiplication factor k_{eff} interpreted as the ratio of the total number of fission neutrons released in consecutive generations. However, in an accelerator driven system, the correspondence between k_λ and k_{eff} is dependent on properties of the spallation target and the core geometry/composition in a nontrivial way. As will be shown, a major part of the power released in a chain reaction is dissipated before the system has had time to relax into the persisting mode. Therefore the eigenflux and the concomitant eigenvalue have only far-fetched correspondence with effective neutron multiplication, and the notation k_{eff} should, in order to maintain a consistent terminology, not be used for the eigenvalue.

Instead we choose to define k_{eff} for sub-critical systems through the following relation:

$$N_f = \frac{k_0}{\nu_0} \frac{1}{1 - k_{eff}} \rightarrow k_{eff} = 1 - \frac{k_0}{\nu_0 N_f} \qquad (2)$$

where k_0 is the ratio n_1/n_0 of the number of neutrons released in fissions induced by external source neutrons (n_1) to the number of source neutrons (n_0), ν_0 is the average (prompt + delayed) neutron yield in these fissions, and N_f is the total number of fissions induced. Thus we have a simple and physically consistent formula connecting power yield (proportional to N_f) with a global parameter characterizing the system (k_{eff}). Using deterministic codes, N_f is easily obtained from the power yield per external source neutron by dividing with the average energy release in an average fission, while in Monte Carlo codes N_f is directly determined by the weight of fissions per source neutron, or alternatively as

$$N_f = \frac{k_0}{\nu_0}(1 + k_1 + k_1 k_2 + k_1 k_2 k_3 + \dots) \qquad (3)$$

where $k_i = n_{i+1}/n_i$, $i > 0$, is the effective neutron multiplication factor of fission generation *i*.

3) METHOD

Neutronics

We used the MCNP Monte-Carlo method [2] in standard mode to simulate the transport of neutrons emerging from the spallation target. Cross sections for the relevant temperatures, i.e. 1200K in regions containing fissile material, 900K in remaining regions, were calculated with NJOY [3] using ENDF/VI room temperature cross sections for U233, Th232 and Pb isotopes, and JEF2.2 room temperature cross sections for fission products and steel

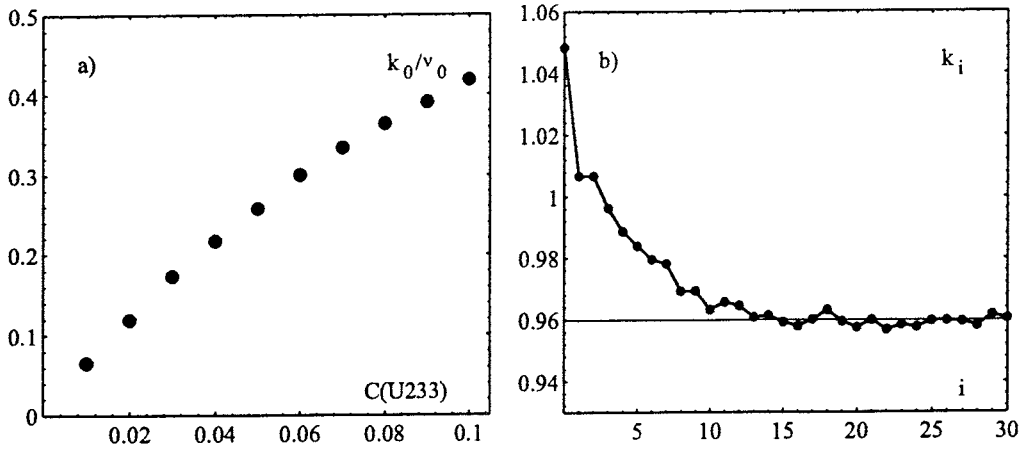

Figure 1:

a) The fraction k_0/ν_0 of source neutrons inducing a fission as function of U233 enrichment.

b) The generation dependent multiplication factor k_i. The track length estimate of k_i given by the MCNP KCODE was used with 50 000 neutrons per fission cycle.

components. The energy release per fission adopted in these data these data was 180.84 MeV for U233, 180.88 MeV for U235 and 171.91 MeV for Th232. The distribution of source neutrons was assumed to be independent of angles, while the energies were sampled from the distribution given in the benchmark instructions (originated from a HETC simulation of the spallation process). The fraction of source neutrons inducing a fission, k_0/ν_0, was determined by setting the numbers of neutrons released in a fission to zero, and is displayed as a function of U233 enrichment in Fig. 1a.

It is to be noted that k_0 is larger than all consecutive k_i, due to slowing down in lead which decreases the probability of capture in thorium and cladding materials. The generation dependent multiplication factors k_i could be found by running MCNP in KCODE mode, and extracting the track length estimate of k_i for individual fission generations. An example of the resulting generation dependence is shown in Fig. 1b. As can be seen, the first 10-15 generations are subject to significantly lower neutron losses than in the asymptotic limit. This can partially be attributed to the probability of a fission neutron to enter the spallation target, where it is allowed to decelerate, avoiding capture in cladding materials and thorium, and then to enter the core again, with a high probability of inducing (epi-thermal) fission in U233. A similar behaviour was seen by Barashenkov, Sosnin and Polanski [4] in a Monte-Carlo investigation of an U238 based ADS. Since the first few k_i:s may be larger than unity, even for deeply sub-critical systems, this phenomenon enhances the power peaking in the vicinity of the target, and should be carefully analyzed in design and safety studies of systems with liquid metal coolant/target.

A further implication of significance is that on average, the chain of fission reactions induced by a single source neutron, has a concomitant neutron flux being distinct from the eigenflux. For example, in Fig. 1b, the number of fissions induced in a fission chain is

$$N_f \frac{\nu_0}{k_0} = \frac{1}{1-k_{eff}} = 31.25 \qquad (4)$$

while the system does not relax into the persisting mode until the 15th fission or so. Thus, half of the fission power is released when the system is not in an eigenstate.

The source importance φ^* of a sub-critical system has been defined as the ratio of fission power to the unphysical power extracted from a neutron flux given by the persisting eigenmode[5,6]. In the framework of the present paper, φ^* can be expressed as

$$\varphi^* = \frac{k_{eff}}{k_\lambda} \frac{1-k_\lambda}{1-k_{eff}} \qquad (5)$$

We note that since the eigenflux has no physical relevance for a significant fraction of the fission power distribution, a source importance defined as in (5) may be misleading. The physical background of an expansion in eigenmodes is that for some systems, a perturbation will lead to the system being in a superposition of well defined eigenstates. If the perturbation (like an external neutron source), is turned off, the contribution of excited eigenstates is damped over time. The neutron flux in a sub-critical system however, does at no point correspond to any of the excited eigenmodes, and thus all physical significance of the eigenmode expansion is lost. For a deeply subcritical system ($k_\lambda < 0.9$), the entire fission chain has come to an end before the flux has relaxed into the persisting mode. Hence it is meaningless to define the source importance as in equation (5). A useful parameter for describing the importance of the external neutron source could be the fraction of power being dissipated before the limit $k_i = k_\lambda$ has been reached. However, a meaningful description of the flux behaviour can only be achieved by explicit plotting of the flux distribution generation by generation.

Averaging over k_i for $i > 20$ we obtained values of k_λ according to the standard procedure of the KCODE. For those runs it was sufficient to average over 80 cycles with 5 000 neutrons tracked per cycle to achieve a statistical error in k_λ (one standard deviation) smaller than 0.0007.

In order to calculate k_{eff} from formula (2), N_f was taken as the weight of fissions per source neutron given by a standard MCNP run. A statistical error of k_{eff} could be estimated via the MCNP parameter M, denoting net neutron multiplication. A relation between M and k_{eff} is obtained by making the following observations:

$$N_f = \frac{G_f}{\nu - 1}$$
$$M = 1 + G_f + G_x \qquad (6)$$

Where G_f is the gain of neutrons in fission reactions and G_x is the neutron gain in (n,xn) reactions. Substitution of (6) into (2) yields the following formula:

$$k_{eff} = 1 - \frac{k_0}{\nu_0} \frac{\nu - 1}{M - (1 + G_x)} \qquad (7)$$

It was checked that (7) gave the same result as the weight of fissions per source neutron, and both values agreed perfectly with KCODE results obtained with (3) for test cases.

Burn-up

The fission product and actinide generation in the ADS was simulated using the ORIGEN2 code [7]. Effective one-group cross sections for capture, fission and (n,xn) reactions in the core regions were calculated with MCNP for 20 actinides and 180 fission products at BOL and an enrichment yielding $k_\lambda = 0.94$. Separate sets were obtained for the inner and outer region of the core, differing by 5-10 % for capture, fission and (n,2n) cross sections, while a difference of an order of magnitude was found for (n,3n) actinide cross sections. This difference can be attributed to the high energy tail of the spallation neutron spectrum, which affects reactions in the center of the ADS. In the appendix a table with values for a selection of isotopes is given. The BOL values were assumed to be valid throughout the entire burn-up. This approximation could be checked by calculating them again at EOL, which however was not yet done.

For isotopes not available in the JEF2.2 library, the ORIGEN cross section library for a sodium cooled Th232 fast breeder enriched with 14% U233 was used. In particular, this concerned Th229, Th231, Pa230 and Pa232 , which appear with non-negligible

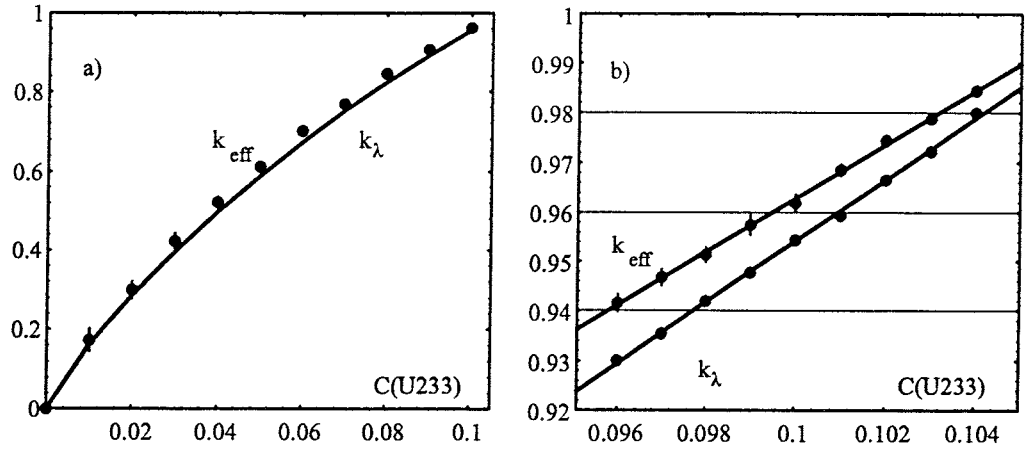

Figure 2:

The eigenvalue k_λ of the neutron transport equation (solid line in a)) and the effective neutron multiplication coefficient k_{eff} as function of U233 enrichment. k_{eff} is generally larger than k_λ, while they converge in the limits k_{eff} -> 0 and k_{eff}-> 1. A linear inter- polation is thus valid only in limited intervalls.

concentrations during burn-up. The ORIGEN2 code does not in itself allow space-dependent treatment of neutron flux. Averaging the flux over the power producing regions of the ADS however leads to a severe under-estimation of the fission product and higher actinide accumulation in the vicinity of the spallation target. This is lethal for the accuracy of the concurrent determination of k_{eff} by means of Monte Carlo simulations, since its value is highly dependent on the first few k_i:s in formula (3). Thus the results of the present benchmark, where averaging was to be made over the entire inner and outer core region, respectively, should in no case be assumed to be valid for a real system.

4) RESULTS

In figure 2 we display the multiplication eigenvalue k_λ and k_{eff} defined according to (2) as functions of the U233 enrichment in the core region. The number of KCODE cycles was 101, with 5000 neutrons per cycle. The first 20 cycles were not used for calculating k_λ, since their inclusion would yield an overestimation of k_λ, and thus a too low value of enrichment for a given k_λ. In the standard mode runs, the number of source neutrons was 10000. The relative (one standard deviation) errors in M was about 0.03, yielding absolute errors around 0.002 for k_{eff}. Since k_{eff} must approach zero for zero concentration of fissile material, a linear interpolation can not be generally valid as seen in figure 2a. In the range of enrichments relevant for the present investigation, it seems that a linear interpolation is acceptable though. Using the linear interpolations shown in figure 2b, we find enrichments of U233 as given in table 1.

k_λ	C(U233)	k_{eff}
0.94	9.771 %	0.9504
0.96	10.095 %	0.9679
0.98	10.419 %	0.9854

Table1: Enrichments of U233 in the core region of the ADS yielding multiplication eigenvalues k_λ = 0.94, 0.96, 0.98

In Figure 3, the effect of voiding the core regions of lead coolant is shown. For voiding only the inner region, a markedly positive change in reactivity is seen, while only a small change is found for voiding of the entire core. However, noting the positive void coefficient in the former case, it is likely that the minor change in the latter is due to two or more physical effects cancelling each other. Hence, it would be valuable to have a more realistic simulation of void effects in the following stage of the benchmark, with the void being gradually introduced in the core, starting both from the centre and from the top. Precise values of the void reactivity effect are tabulated in the appendix.

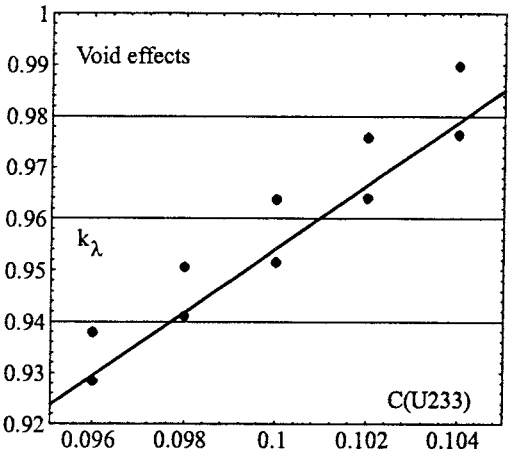

Figure 3:

Effects of voiding the core regions of lead coolant. Solid line: linear interpolation of k_λ for the unvoided system, see Fig 2b. Points above solid line: k_λ in the case of voiding of the inner core region of lead. Points below solid line: k_λ for voiding of the entire core region. Numerical values of void coefficients are tabulated in the appendix.

The source importance as defined by equation (5) was calculated from the linear interpolations shown in Figure 2b, and is displayed in Figure 4, with numerical values given in the appendix. It is to be noted that the linear interpolations are valid only in a limited interval, and thus the apparently monotonic growth of φ^* is not a global characteristic. Actually, in the limit k_{eff} -> 1, φ^* must approach a constant value:

$$\lim_{k_{eff}->1^-} \varphi^* = \lim_{k_{eff}->1^-} \frac{k'_\lambda}{k'_{eff}} \qquad (8)$$

as can be seen from making a Taylor expansion of (5). Unfortunately the computation time for calculating k_{eff} in the vicinity of criticality becomes too large for numerical examplification of formula (8).

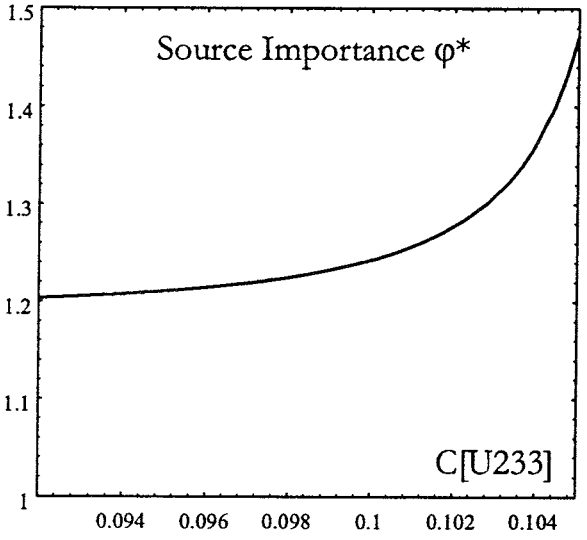

Figure 4:

The source importance φ^* as function of U233 enrichment, defined as in equation (5). The plotted values were obtained using the linear interpolations in Figure 2b. The monotonic growth is only present in the displayed intervall. In the criticality limit φ^* will approach a constant value.

The ratio of spectrum averaged fission cross sections, $<\sigma_f(Th233)/\sigma_f(U233)>$ for k_λ = 0.96 is shown in figure 5 as function of radius. This ratio can be thought of as a spectral index with a higher value indicating a harder spectrum. The values were calculated by taking the average over a 10 cm wide concentric disc. As seen, the spectrum apparently is harder in the outer core region, which supports the hypothesis of fission neutrons in the inner region being able to "relax" in the spallation target before re-entering the core. A tabulation of numerical values for k_λ = {0.94,0.96,0.98} is given in the appendix.

The radial power distribution at mid-plane was calculated from the power density per source neutron given by MCNP by multiplying with the source intensity needed to achieve a total fission power of 1500 MW. Results are plotted in figure 6. Numerical values of radial and axial power distributions are given in the appendix.

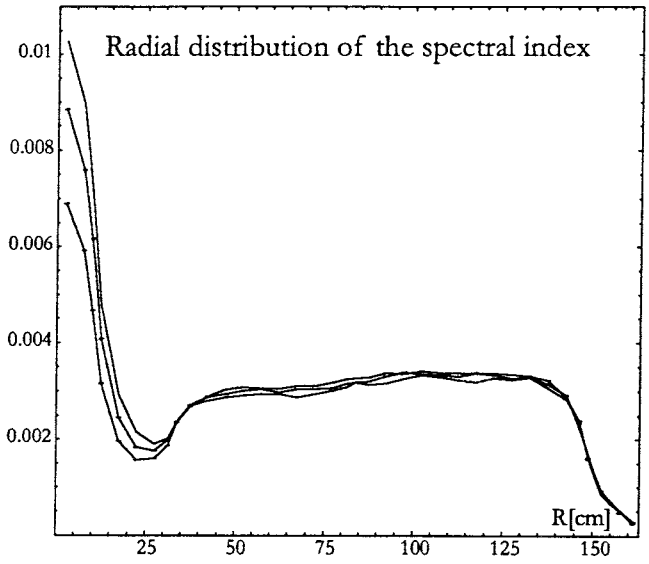

Figure 5:

The ratio of spectrum averaged fission cross sections, $<\sigma_f(Th233)/\sigma_f(U233)>$, as function of radial position along the mid-plane of the core for $k_\lambda = 0.94$ (larger at origin), $k_\lambda = 0.96$ (intermediate at origin) and $k_\lambda = 0.98$ (smaller at origin). Numerical values are tabulated in the appendix.

The time dependence of the multiplication eigenvalue k_λ is displayed in figure 7 for $k_\lambda = 0.94$ and $k_\lambda = 0.96$. During the first 150 days the reactivity changes quickly due to fissioning of U233, while the supply of U233 through breeding is delayed. Therefore a time step of 50 days was used in this region, while a 150 day step was assumed for the remaining part. A control calculation using the larger time grid also for the initial step was made, and it was found that k_{eff} at t = 150 days became under estimated by at least 400 pcm, which is outside the statistical error. The change in k_λ was smaller, as its value is less sensitive to the composition in the inner core region. Hence, the choice of time grid in the initial phase may be a cause of differences in the time dependence of source intensity calculated by different groups.

The increase in reactivity obtained when removing all fission products at t = 900 days (corresponding to a decrease in atomic density of about two percent) was found to be around 2200 pcm for k_λ [BOL] = 0.94, and 2500 pcm for k_λ [BOL] = 0.96.

The output data from MCNP:s KCODE were interpolated with 2nd order splines for t < 150 days, and fitted with a 3rd order polynomial for t > 150 days. The values of k_λ given in the appendix are inferred from the polynomial fits, in order to suppress errors deriving from the Monte Carlo procedure.

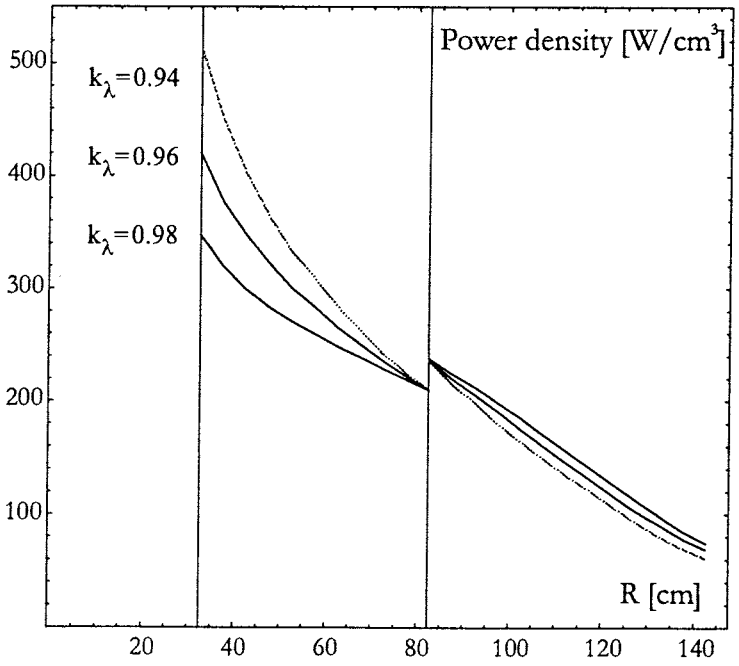

Figure 6:

Radial distribution of power densities, in units of W/cm^3. The intensity of the external neutron source is adjusted in order to obtain a total fission power of 1500 MW. The power peaking in the vicinity of the target is due both to the localized external neutron source, as well as inelastic slowing down of fission neutrons in the target.

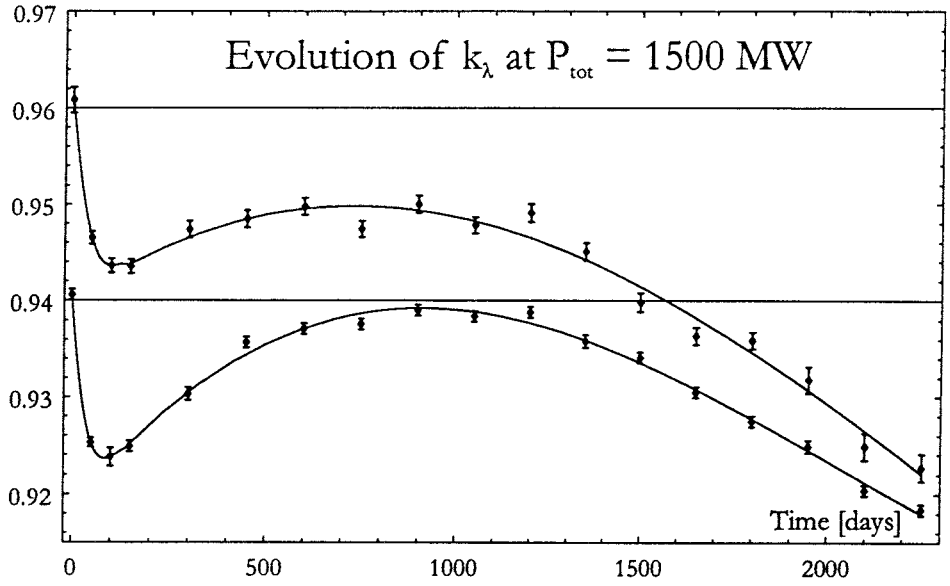

Figure 7:

Evolution of the multiplication eigenvalue k_λ as function of time asuming that the external neutron source is adjusted to maintain a 1500 MW fission power output in the core. The solid lines represent third order polynomial fits. The values tabulated in appendix are inferred from the fits, in order to suppress the error deriving from the Monte Carlo process.

The external neutron source intensity needed to sustain a total fission power of 1500 MW is shown in figure 8. It was calculated as the ratio of the total fission power (1500 MW) to the power per source neutron given by MCNP. Tabulated values are again inferred from a polynomial fit.

The activity of the core region materials following EOL and shut-down of the external neutron source was calculated with ORIGEN2, with results given in table 2. The values for k_λ [BOL] = 0.98 were found by approximating the neutron flux during the entire burn-up with the flux at BOL.

Time [years]	10^2	10^3	10^4	10^5	10^6
k_λ(BOL) = 0.94	6.02 10^9	6.79 10^7	2.07 10^8	2.26 10^8	7.06 10^6
k_λ(BOL) = 0.96	6.02 10^9	6.85 10^7	2.09 10^8	2.28 10^8	7.11 10^6
k_λ(BOL) = 0.98	5.82 10^9	6.92 10^7	2.11 10^8	2.30 10^8	7.11 10^6

Table 2: Specific activity of the ADS fuel following EOL, in units of Bq/g.

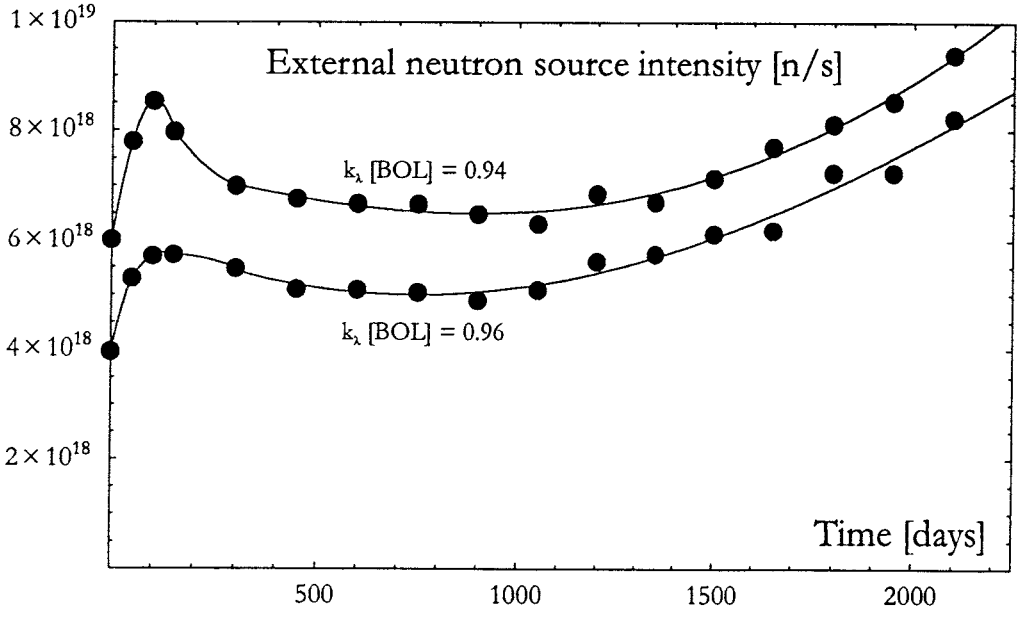

Figure 8:

The external neutron source intensity necessary to maintain a constant fission power of 1500 MW during burn-up. The solid lines represent third order polynomial fits. The values tabulated in appendix are inferred from the fits, in order to suppress the error deriving from the Monte Carlo process.

5) CONCLUSIONS

By making a definition of the effective multiplication factor k_{eff} that is strictly related to the number of fissions per external source neutron (2), we have obtained a global parameter characterizing a sub-critical system with physical meaning. Explicit calculations show that the transient period in the chain of fissions corresponds to a significant part of the power released in the system, and that the asymptotic flux is not achieved until the 15th fission generation (for $k_\lambda = 0.96$). In deeply sub-critical systems ($k_\lambda < 0.9$), the asymptotic flux is *never* reached. Therefore we argue that neither the asymptotic flux nor the multiplication eigenvalue should be used as a frame of reference in a self consistent theoretical treatment of such systems. A source importance defined as in (5,6), for instance, does not fulfill conditions that one would like to impose on such a parameter, like being infinite (or alternatively equal to unity) in the limit of zero neutron multiplication, and zero in the criticality limit.

Consequently, when calculating multiplication eigenvalues using a Monte Carlo code like the MCNP KCODE, averaging over steady-state generations should commence no earlier than in the 15th generation, if one uses the external source for the first fission generation.

The calculation of void effects show that reactivity coefficients can be markedly positive for a lead cooled system if only partial voiding takes place. For a better understanding of this phenomenon, calculations for a gradual voiding of the ADS starting from the top (as is physically relevant) are desired.

We would like to point out that the introduction of an extended target volume leads to deceleration of fission neutrons entering the target. These neutrons thereby avoid resonance capture in cladding materials, and induce fission in U233 with a higher probability than neutrons not entering the target. This phenomenon gives an additional contribution to the power peaking in the vicinity of the target, and should be carefully analyzed when optimizing the size of the target region. Note that this moderating property of lead is in apparent contradiction to ideas of "adiabatic resonance crossing" applied to transmutation of fission products (8).

Regarding the simulation of burn-up, we believe that a finer grid with respect both to space and time is mandatory for achieving realistic modelling of an ADS with significant flux gradients in the core. In any case such grids must be well defined in a benchmark like the present.

6) ACKNOWLEDGMENTS

The authors are grateful for financial support from the Swedish Nuclear Fuel and Waste Management Board and the Centre of Nuclear Technology.

7) REFERENCES

[1] H. Takahashi, Fusion technology **20** 657 (1991).

[2] MCNP - A general Monte Carlo N-Particle transport code, version 4A, LA-12625-M. Editor J. F. Briesmeister. Los Alamos National Laboratory (1993).

[3] The NJOY nuclear data processing system, version 91, LA-12740-M. Editors R.E. MacFarlane and D.W. Muir. Los Alamos National Laboratory (1994).

[4] V. Barashenkov, A. Sosnin, and A. Polanski, Nuclear methods for transmutation of nuclear waste, proceedings of the International workshop in Dubna (1996), p.77.

[5] V. Seliverstov, Proceedings of the second international conference on Accelerator-Driven Transmutation Technologies and Applications, editor Henri Condé, Uppsala University (1997), p. 891.

[6] M. Salvatores et al., Proceedings of the second international conference on Accelerator-Driven Transmutation Technologies and Applications, editor Henri Condé, Uppsala University (1997), p. 513.

[7] A. Croff, Nuclear Technology **62** 335 (1983).

[8] C. Rubbia et al. Fast neutron incineration in the energy amplifier as an alternative to geologic storage: The case of Spain. CERN/LHC/97-01 (1997).

APPENDIX

k_λ	VE reg. 1	VE reg. 2
0.94	938	-138
0.96	1011	-211
0.98	1081	-281

Table 3: Void Effects for the multiplication eigenvalue [pcm]

k_λ	φ^*	$P_{max}(1)/P_{max}(2)$
0.94	1.22	2.18
0.96	1.26	1.78
0.98	1.38	1.46

Table 4: Source importance and ratio of maximal power densities at EOL

z [cm]	$k_\lambda = 0.94$	$k_\lambda = 0.96$	$k_{\lambda = 0.98}$
0	402.2	347.5	299.3
10	393.4	337.6	292.9
20	377.9	325.2	284.7
30	347.8	302.9	266.4
40	313.8	273.8	242.0
50	276.9	242.8	218.0
60	239.0	213.7	194.5
70	212.7	196.3	180.8

Table5: Axial power distrubtion [W/cm³] at R = 42.5 cm.

z [cm]	$k_\lambda = 0.94$	$k_\lambda = 0.96$	$k_\lambda = 0.98$
0	61.1	69.3	74.5
10	61.1	67.3	74.0
20	59.7	64.2	71.6
30	56.6	62.5	68.2
40	53.3	58.6	63.1
50	48.9	52.5	58.0
60	45.7	49.0	53.0
70	47.0	50.5	53.7

Table6: Axial power distribution [W/cm³] at R = 142.5 cm.

R [cm]	k_λ= 0.94	k_λ= 0.96	k_λ= 0.98
33.0	513.6	420.3	347.5
37.5	449.8	376.7	319.6
42.5	402.2	347.5	299.3
47.5	364.3	322.8	283.8
52.5	332.6	300.5	270.8
57.5	309.4	284.1	259.7
62.5	284.3	265.5	248.2
67.5	263.0	249.9	238.5
72.5	241.5	235.0	228.2
77.5	224.4	221.8	218.6
82.0	209.8	209.0	209.1
83.0	235.3	236.5	237.3
87.5	214.6	219.4	223.8
92.5	198.0	204.8	211.8
97.5	179.8	190.5	198.1
102.5	164.2	174.9	184.9
107.5	149.1	160.1	170.0
112.5	134.3	145.5	155.8
117.5	121.0	131.3	141.3
122.5	107.0	116.8	126.8
127.5	93.0	102.7	112.6
132.5	80.3	90.9	98.7
137.5	70.0	78.4	85.2
142.5	61.1	69.2	74.5

Table7: Power density at mid-plane [W/cm^3] as function of radius R.

R [cm]	k_λ= 0.94	k_λ= 0.96	k_λ= 0.98
2.5	10.270	8.843	6.898
7.5	8.948	7.588	5.921
12.5	4.784	4.071	3.155
17.5	2.930	2.454	1.962
22.5	2.156	1.827	1.565
27.5	1.898	1.755	1.592
32.5	2.190	2.174	2.103
37.5	2.702	2.707	2.681
42.5	2.796	2.879	2.894
47.5	2.869	2.940	3.031
52.5	2.910	3.007	3.080
57.5	2.939	3.040	3.055
62.5	2.936	2.973	3.049
67.5	2.870	3.036	3.104
72.5	2.934	3.041	3.102
77.5	3.007	3.063	3.174
82.5	3.122	3.163	3.253
87.5	3.126	3.195	3.281
92.5	3.158	3.305	3.373
97.5	3.254	3.388	3.355
102.5	3.324	3.344	3.408
107.5	3.283	3.334	3.375
112.5	3.224	3.297	3.374
117.5	3.183	3.368	3.379
122.5	3.268	3.340	3.371
127.5	3.234	3.265	3.346
132.5	3.280	3.287	3.313
137.5	3.068	3.150	3.228
142.5	2.842	2.930	2.898
147.5	1.992	1.969	2.005
152.5	0.850	0.937	0.929
157.5	0.478	0.473	0.477
162.5	0.239	0.183	0.214

Table 8: Radial distribution of the spectral index $<\sigma_f(Th233)/\sigma_f(U233)>$ [10^{-3}].

Time [days]	$k_\lambda = 0.94$	$k_\lambda = 0.96$
0	0.9400	0.9600
150	0.9251	0.9438
300	0.9305	0.9466
450	0.9344	0.9484
600	0.9371	0.9495
750	0.9387	0.9498
900	0.9392	0.9493
1050	0.9389	0.9482
1200	0.9377	0.9465
1350	0.9359	0.9442
1500	0.9336	0.9414
1650	0.9308	0.9382
1800	0.9277	0.9346
1950	0.9245	0.9307
2100	0.9212	0.9265
2250	0.9179	0.9221

Table 9: Evolution of the multiplication eigenvalue over time.

Time [days]	$S_{0.94}$	$S_{0.96}$
0	6.01	3.96
150	7.97	5.74
300	7.00	5.45
450	6.79	5.18
600	6.63	5.04
750	6.53	5.00
900	6.50	5.04
1050	6.54	5.18
1200	6.66	5.40
1350	6.87	5.69
1500	7.16	6.05
1650	7.56	6.48
1800	8.05	6.97
1950	8.65	7.51
2100	9.37	8.10

Table 10: Evolution of the external neutron source intensity [10^{18} n/s]

Isotope	σ_c (barns)	$\sigma_{(n,2n)}$ (barns)	$\sigma_{(n,3n)}$ (barns)	σ_f (barns)
230Th	1.844E-01	8.858E-04	1.019E-05	2.557E-02
232Th	3.509E-01	8.910E-04	2.595E-05	7.435E-03
231Pa	2.984	5.986E-04	1.072E-05	2.366E-01
233Pa	1.018	2.439E-04	1.923E-05	5.203E-02
232U	6.613E-01	4.559E-04	1.549E-05	2.152
233U	2.693E-01	2.992E-04	1.602E-06	2.703
234U	5.833E-01	8.948E-05	5.530E-06	3.943E-01
235U	5.134E-01	6.267E-04	5.845E-06	1.859
236U	5.414E-01	4.326E-04	1.971E-05	1.265E-01
237U	4.514E-01	1.244E-03	2.757E-05	6.192E-01
238U	3.269E-01	6.248E-04	1.796E-05	3.396E-02
237Np	1.507	1.336E-04	3.235E-06	3.113E-01
238Np	1.663E-01	7.979E-04	1.350E-05	3.467
238Pu	5.281E-01	4.365E-05	2.057E-06	1.102
239Pu	4.979E-01	1.785E-04	1.785E-04	1.800
240Pu	5.706E-01	2.121E-04	8.617E-06	3.701E-01

Table 11: Effective one-group cross sections in the inner core region at BOL.

Isotope	σ_c (barns)	$\sigma_{(n,2n)}$ (barns)
83Kr	2.659E-01	3.037E-04
84Kr	3.801E-02	3.774E-05
86Kr	5.494E-03	4.782E-05
85Rb	1.843E-01	0
87Rb	1.662E-02	0
88Sr	1.079E-03	0
90Sr	1.366E-02	0
89Y	2.135E-02	2.913E-05
91Zr	6.540E-02	1.964E-04
92Zr	3.944E-02	0
93Zr	1.019E-01	3.642E-04
94Zr	2.435E-02	0
96Zr	3.055E-02	3.021E-04
95Mo	2.983E-01	0
97Mo	2.976E-01	0
98Mo	9.506E-02	1.889E-04
100Mo	7.418E-02	2.421E-04
99Tc	5.718E-01	1.760E-04
100Ru	1.787E-01	0
101Ru	6.416E-01	5.007E-04
102Ru	1.500E-01	0
104Ru	1.327E-01	0
103Rh	6.087E-01	1.295E-04
128Te	3.251E-02	0
130Te	1.410E-02	0
127I	5.513E-01	1.578E-04
129I	3.210E-01	1.499E-04
131Xe	2.823E-01	9.862E-04
132Xe	6.788E-02	1.922E-04
134Xe	3.687E-02	2.477E-04
136Xe	2.846E-03	2.922E-04
133Cs	4.355E-01	1.913E-04

135Cs	6.709E-02	0
137Cs	2.231E-02	1.848E-04
138Ba	3.509E-03	1.851E-04
139La	3.197E-02	2.046E-04
140Ce	1.417E-02	0
142Ce	3.937E-02	5.178E-04
144Ce	3.911E-02	7.234E-04
141Pr	1.140E-01	1.357E-04
143Nd	2.725E-01	1.274E-03
144Nd	6.260E-02	4.136E-04
145Nd	4.618E-01	1.961E-03
146Nd	8.412E-02	5.100E-04
148Nd	1.267E-01	6.721E-04
148Sm	3.192E-01	0

Table 12: Effective one-group cross sections for the most abundant fission products in region 1.

Transmutation of ^{137}Cs and ^{129}I using a muon catalyzed fusion neutron source

Jan Wallenius

Department of Nuclear & Reactor Physics

Royal Institute of Technology

S-100 44 Stockholm, Sweden

Phone:+46 - 8 - 790 6395

Fax:+46 - 8 - 10 69 48

E-mail: janne@neutron.kth.se

Abstract

Transmutation of the radiotoxic isotopes ^{137}Cs and ^{129}I using a muon catalyzed fusion (μCF) neutron source is considered. Extensive Monte Carlo simulations show that each fusion neutron may transmute up to 1.7 radiotoxic nuclei, depending on geometry and choice of material. Further, it is found that chemically confining Cesium atoms in the compund Cs_2O leads to higher transmutation efficiency for a given volume as compared to pure Cesium.

Assuming that a minimal requirement for applying transmutation to ^{137}Cs is that the inventory half-life with respect to undergoing transmutation is less than twice the natural half-life $T_{1/2}$ = 30 years, the highest transmutation rate in a system consisting of a μCF source with a maximum achievable intensity of $5*10^{18}$ n/s , is ~5 kilograms per year, at an inventory of 300 kilograms. For larger inventories, the half-life becomes longer. Hence, it seems difficult to achieve a positive energy balance in the process, in contradiction with results of a previous study.

I) INTRODUCTION

The possibility of transmuting high-level radioactive waste from nuclear power plants by means of accelerator supported neutron sources was suggested over 30 years ago [1]. In the late eighties these ideas were developed into a mature state by H. Takahashi and co-workers at Brookhaven National Laboratory [2]. The transmutation process is generally conjectured as the utilization of a neutron surplus in a sub-critical breeding system, which allows for a significant amount of neutron captures in fission products and minor actinides without ruining the neutron economy of the system. For fission products, the neutron capture process is usually regarded as the operative transmutation reaction. For instance, one has

$$n + {}^{137}Cs \rightarrow \gamma + {}^{138}Cs \rightarrow {}^{138}Ba + \beta^- \qquad (1)$$

with a half-life of the ^{138}Cs β-decay channel equal to 32 minutes, compared to the natural decay of ^{137}Cs with a half-life of 30 years. However, the effective cross section of reaction (1) is comparatively small for different types of fissile multiplying cores having either thermal [3] or fast [4] spectra, leading to the necessity of very large neutron fluxes ($\sim 10^{16}$ s^{-1} cm^{-2}) for the transmutation rate of fission products to become significant.

Therefore, the suggestion to use a muon catalyzed fusion neutron source to transmute ^{137}Cs by means of the (n,2n) reaction deserves some attention [5]. The (n,2n) reaction has a cross section which is of the order of a barn for fission products and neutron energies above 9 MeV. Applying it to ^{137}Cs one has

$$n + {}^{137}Cs \rightarrow 2n + {}^{136}Cs \rightarrow 2n + {}^{136}Ba + \beta^- \qquad (2)$$

with a half-life of the ^{136}Cs β-decay channel equal to 13 days. For a pure DT-fusion spectrum where neutrons have an initial kinetic energy of 14.1 MeV, one can expect a high transmutation efficiency applying reaction (2). In reality, the fusion spectrum will be degraded by interactions with the DT-gas and container walls even before entering the transmutation region, where additional slowing down will take place due to elastic and in-elastic scattering.

The present investigation aims to clarify the impact of competitive processes in the μCF based transmutation of fission products, as well as to optimize some geometric properties of the DT fusion cell and the Cesium container. This is achieved by extensive Monte-Carlo simulations of the neutron flux using MCNP [6], as will be accounted for in the following section. The macroscopic cross section of reaction (2) is dependent on the chemical form chosen for the Cesium content and in section three it is shown that CsI and Cs_2O are compounds that besides being chemically less agressive than pure Cesium also feature higher Cesium densities than the pure element does and therefore yield higher transmutation efficiencies at a fixed volume. In section four the Cs_2O compund is used as a basis for calculating thetransmutation rate for different amounts of the radiotoxic isotope. Assuming realistic values for deuteron beam intensities, pion multiplicity and pion to muon conversion factors, the transmutation rate of ^{137}Cs in kg/year is calculated. Finally some remarks on the economical viability of the present scheme are given.

II) MONTE-CARLO SIMULATIONS OF NEUTRONICS

The neutronics of the μCF based system for transmutation was simulated with version 4B of MCNP [6]. A geometrical setup was made as follows: The DT-fusion cell was assumed to be a cylinder of 50 cm length and variable radius. The DT-container was taken to be made of 1 cm thick

titanium in order to withstand the pressure of the high-denisty DT-gas. The DT-gas was assumed to have equal proportions of D_2 and T_2 molecules, and to have a density equal to half of Liquid Hydrogen Density (1 LHD = $4.25*10^{22}$ atoms/cm^3). This density is necessary to obtain a desired neutron multiplicity of 100 per muon [7]. The Cesium container was assumed to be constructed in Zirconium, having a thickness of 0.5 cm. It was supposed to have the shape of a sphere with a cylindrical hole in the middle for fitting the DT-container. The radius of the cylindrical hole was fixed to 14.5 cm, while the radius of the sphere was varied from 30 cm up to 200 cm.

Cross sections for neutron scattering on ^{2}H, ^{3}H, ^{22}Ti, ^{40}Zr, ^{16}O, ^{129}I and ^{137}Cs were calculated at 900 K with NJOY [8] using room temperature cross sections from the JEF2.2 library. Data for the (n,2n) cross section for ^{137}Cs were missing, but could be added from the EAF compilation [9]. In Figure 1 this cross section is plotted, together with JEF2.2 data for ^{129}I.

In order to investigate the degrading of the fusion spectrum the fraction of neutrons having an energy above/below the reactive limit 9 MeV was sampled. The source neutrons were assumed to be equally distributed in the fusion cell, and the cylindrical radius was increased from 1 to 10 cm. As shown in Figure 2, a significant fraction of the neutrons falls below the 9 MeV threshold already within the DT-gas, increasing with approximately one percent per one cm increase in radius. During transport through the titanium container an additional 10 percent falls below the threshold, and eventually the fraction of high energy neutrons entering the Cesium mixture is down to 78 % for a fusion cell with 10 cm cylindrical radius. These numbers show that the "pure" 14 MeV neutron source based on muon catalyzed fusion suggested in reference [7] is contaminated by a low-energy tail constituting at least 15-20% of the fluence, due to inelastic scattering in titanium and hydrogen.

III) TRANSMUTATION EFFICIENCY

The previous study of the transmutation efficency of a μCF neutron source [5] considered only pure ^{137}Cs as target for the fusion neutrons. Cesium is an akali metal, and is therefore chemically agressive. Further, its density becomes comparatively low, having a value of 1.87 g/cm^3. The mean free path of a fusion neutron in a ^{137}Cs is as large as 25 cm. However, several chemical Cesium compounds have a density above 4 g/cm^3, and may therefore be interesting candidates for the purpose of transmuting ^{137}Cs. Here, the salt CsI and the oxide Cs_2O are investigated, the former due to the possibility of simultaneous transmutation of the long lived isotope ^{129}I, the latter due to its high effective Cs density ~ 3.2 g/cm^3.

For definiteness, the cylindrical radius of the DT-cell is fixed to 5 cm, yielding an initial neutron fraction able to induce (n,2n) reactions in the transmutation chamber of 81 %. The radius of the sphere containing material to be transmuted is then varied between 30 and 200 cm. Results for the three different compositions are outlined in Figures 3-4.

In the case of pure ^{137}Cs, one finds that the fraction of source neutrons inducing (n,2n) reactions is ~6% at a radius of 30 cm, growing to ~60% at a radius of 200 cm. Additional calculations for larger radii show that the fraction saturates at ~71%. Noting that the initially available fraction was 81 %, one concludes that the (n,2n) transmutation efficiency is very high. Since all neutrons born in the transmutation chamber either undergo capture or escape, one finds that the upper limit of the transmutation efficiency η_{tr}, defined as the number of transmutations, i.e. the sum of (n,2n) and (n,γ) reactions per source neutron is

$$\eta_{tr} < 1.7 \qquad (3)$$

in the limit of infinite radius. Note that the fraction of neutrons escaping the transmutation chamber for good with energies above the 9 MeV threshold is larger than the fraction that induced (n,2n) reactions all the way out to a radius of 100 cm.
Substituting the chamber content with Cs_2O with a density of 4.25 g/cm^3 (Cs density ~3.2 g/cm), one finds that the fraction of ^{137}Cs nuclei being transmuted by (n,2n) reactions grows to 12 % at 30 cm radius, and saturates at 55% for large radii. Note that due to moderating properties of oxygen, saturation occures already at R = 200 cm, and that a significant amount of transmutations due to capture in ^{137}Cs appears already at small radii, as compared to the case of pure Cesium. The transmutation efficiency for infinite radius is slightly lower than for pure Cesium, $\eta_{tr} < 1.55$, while it is significantly higher for R < 200 cm.

Filling the chamber with a CsI salt with a density of 4.51 g/cm^3 (Cs density ~2.3 g/cm^3), the mean free path for fusion neutrons is down to 9 cm, and the high energy fraction escaping the chamber becomes negligible at 150 cm radius. The fraction of source neutrons inducing (n,2n) transmutation reactions saturates at 70 %. Further, resonance captures in ^{129}I become abundant at larger radii. In the limit of infinite radius, $\eta_{tr} < 1.70$.

IV) CONSTRAINTS ON THE NEUTRON SOURCE

In order to estimate upper bounds on the transmutation rate, we adopt a deuteron beam current of I_d = 100 mA, which is the highest current of a super conducting linac that is regarded as being realistic, considering constraints on beam pipe and beam window materials [10]. According to recent studies, the optimal pion production target is a graphite cylinder of 5 cm radius and 150 cm length, which will yield 0.22 pions per GeV and deuteron in the beam energy range 2-4 GeV [11]. The pion to muon conversion efficiency $\eta_{\pi\mu}$ is highly system dependent. For a larger fusion cell it may be as high as 0.7 [12]. For smaller cells, like the one here considered, it is reduced to 0.05-0.10 [7,13,14]. A larger fusion cell inevitably will lead to smaller fraction of fusion neutron with energies above the reactive threshold exiting the DT-cell, as well as too large trititum inventories. The DT-cell suggested in reference [12], for instance, contains over 100 kilograms of tritium, which is an order of magnitude above the annual production of the isotope in the world today. Hence $\eta_{\pi\mu}$ = 0.1 is assumed for the present study as a realistic upper limit. Adopting $\eta_{\mu n}$ = 100 as the number of fusions induced per muon [7] and a beam energy E_b = 4 GeV, one arrives at a maximal neutron source intensity $I_n \sim 5*10^{18}$ s-1. The transmutation rate is then given by the following formula:

$$\lambda_{tr} = I_d \, \eta_{d\pi} \, \eta_{\pi\mu} \, \eta_{\mu n} \, \eta_{tr} = I_n \, \eta_{tr} \qquad (4)$$

where η_{tr} is a function of transmutation chamber radius (or equivalent Cesium mass). Cleaning of barium oxide is supposed to take place frequently enough for η_{tr} to be unchanged over time (i.e. ~ once a year). In Table 1 values of η_{tr} and λ_{tr} are displayed in the case of a Cs_2O inventory, for maximal beam intensity and a selection of radii.
Let us assume that a minimal requirement (from the physical viewpoint) for applying transmutation to ^{137}Cs is that the half-life with respect to undergoing transmutation is equal to twice the natural half-life $T_{1/2}$ = 30.2 years. This leads to the condition $2T_{1/2} \lambda_{tr} > m_{Cs}$. As can be seen from Table 1, this is fulfilled only for the smallest inventory here investigated. Thus one finds that the maximal amount of ^{137}Cs that can be transmuted in the present scheme is of the order of five kilograms per year, at an initial inventory of ~300 kilograms.

V) ECONOMICAL REMARKS

The energy cost for a single transmutation in the above case is given by

$$E_{tr} = E_b / (\eta_{acc}\, \eta_{d\pi}\, \eta_{\pi\mu}\, \eta_{\mu n}\, \eta_{tr}) \quad (5)$$

where $\eta_{acc} = 0.5$ stands for accelerator efficiency. Since $\eta_{d\pi}$ is approximately proportional to E_b in the range 2-4 GeV:$\eta_{d\pi} = 0.22\, E_b$ where E_b is expressed in GeV, one has

$$E_{tr} = 1 / (0.11\, \eta_{\pi\mu}\, \eta_{\mu n}\, \eta_{tr}) \quad (6)$$

Assuming $\eta_{\pi\mu} < 0.10, \eta_{\mu n} = 100$ as above, and $\eta_{tr} = 0.11$ for an initial mass of 300 kilograms and 30 cm of radius (see Table 1), the energy cost becomes

$$E_{tr} > 8.0 \text{ GeV} \quad (7)$$

which is to be compared with the energy produced in a LWR per ^{137}Cs waste atom, being 3.3 GeV thermal energy, i.e. ~ 1.0 GeV electric [5]. Thus the energy cost for transmutation of a ^{137}Cs nucleus in the present scheme is, even in the most optimistic case, significantly larger than the energy gain in its production. Taking into account additional expenses for separating the radiotoxic isotopes from the fission product waste stream makes the energy balance to look even worse. This fact does not change when taking into account the fusion energy dissipated in the DT- and the transmutation chamber, which amounts to less than one tenth of the beam energy. Therefore it seems like transmutation of ^{137}Cs based on a muon catalyzed fusion source is not economically viable. This conclusion is in contradiction with reference [5], partailly due to unrealistically optimistic estimations of the deuteron to pion to muon conversion factors.
However, the scheme here presented offers a minor actinide free method for transmutation of troublesome Long Lived Waste like ^{99}Tc, ^{129}I and ^{135}Cs, which might be of interest for countries that have decided to phase out nuclear power.

VI) CONCLUSIONS

The present Monte Carlo simulations show that, due to inelastic scattering in hydrogen and titanium, 15-20 % of the fusion neutrons exiting a muon catalyzed fusion cell had energies below 9 MeV. Therefore is does not seem to be possible to construct a "pure" 14 MeV neutron source as suggested in reference [7].
Transmutation efficiencies were shown to be higher (for transmutation chamber radii smaller than 200 cm) if the Cesium was contained in a chemical compund, like CsI and Cs_2O, with the latter being optimal from the viewpoint of ^{137}Cs transmutation. In pure ^{137}Cs and in a a CsI salt up to 1.7 transmutations per source neutron can be achieved for an infinite radiotoxic isotope volume, while in Cs_2O 1.55 transmutations is the upper limit.
The transmutation rate of ^{137}Cs was found to be ~50 kg/year for a sphere of 200 cm radius. The maximal amount of ^{137}Cs that can be transmuted under the condition that the transmutation half-life is equal to twice the natural half-life, was found to be ~5 kilograms per year. This is an upper limit that in reality may be lowered due to system dependent pion to muon conversion efficiencies and problems with separating ^{137}Cs from other Cesium isotopes in the nuclear waste.
Finally it was shown that even in the most optimistic case, the energy balance of the transmutation process is strictly negative, in contradiction with results of previous works, where deuteron to muon conversion factors seems to have been over-estimated.

ACKNOWLEDGEMENTS

The author would like to express his sincere thanks to Adam Soltan for preparing the cross section

files. This work was supported by the Swedish Nuclear Fuel and Waste Management Board.

REFERENCES

[1] M. Steinberg, G. Watsak, B. Manowitz, Neutron Burning of Long-Lived Fisson Products for Waste Disposal, Brookhaven National Laboratory Report BNL-8558, (1964).

[2] H. Takahashi, Fusion technology **20**, 657 (1991).

[3] C. Bowman et al, Nuc. Inst. Meth. **A** 320, 336 (1992).

[4] C. Rubbia, in Proc. Int. Conf. on Accelerator Driven Transmutation Technologies and Applications, AIP Conference Proceedings **346**, editors E. Arthur, A. Rodrigues and S. Schriber, 44 (1994).

[5] T. Kase et al, Muon Catalyzed Fusion **6**, 521 (1991).

[6] MCNP - A general Monte Carlo N-Particle transport code, version 4B, LA-12625-M Editor J.F. Briesmeister. Los Alamos National Laboratory (1997).

[7] C. Petitjean et al, Fusion technology **25**, 437 (1994).

[8] The NJOY nuclear data processing system, version 91, LA12740-M. Editors R.E. MacFarlane and D.W. Muir. Los Alamos National Laboratoty (1994).

[9] J. Kopeckey and D. Nierop, The European Activation File EAF-4, ECN-C-95-072, Netherlands Energy Research Foundation (1995).

[10] V. Andreev et al, in Proc. Int. Conf. on Accelerator Driven Transmutation Technologies and Applications, editor Henri Condé, Uppsala University, 1020 (1997).

[11] L. Latysheva, I. Psenichnov and M. Vecchi, Hyperfine Interactions **101/102**, 669 (1996).

[12] K. Kataoka, T. Yamasaki and Y. Oka, Fusion Engineering and Design **19**, 111 (1992).

[13] F. Karmanov and D. Naberezhnev, Hyperfine Interactions **101/102**, 677 (1996).

[14] Y. Petrov and E. Sakhnovsky, Hyperfine Interactions **101/102**, 647 (1996).

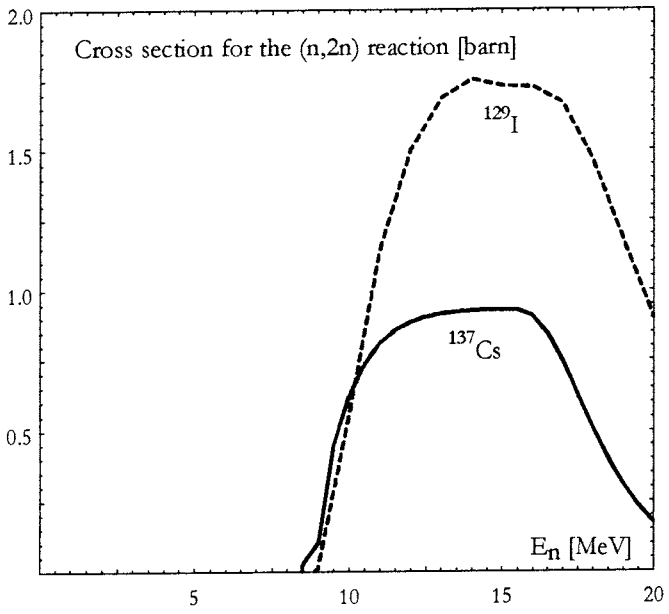

Fig. 1: Cross sections for the (n,2n) reaction in units of barns, plotted by MCNP version 4B with data taken from ENDF/B-VI (^{129}I) and EAF (^{137}Cs) evaluations.

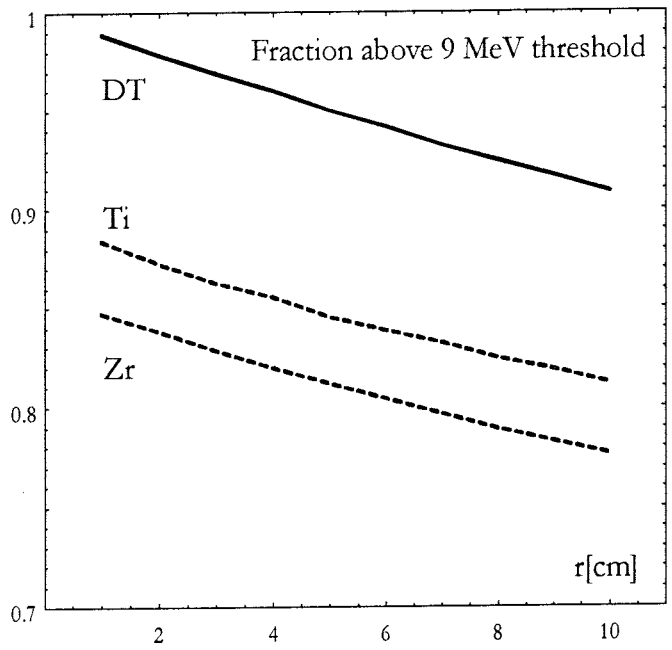

Fig. 2: The fraction of fusion neutrons with energies above the (n,2n) reaction threshold at 9 MeV when exiting the DT mixture (solid line), when exiting titanium container (upper dashed line), and when entering the radiotoxic isotope container after having passed its inner wall (lower dashed line). Values are given as function of the cylindrical radius r of the titanium container inner wall. The distribution of source neutrons was assumed to be uniform within the DT-mixture. The thickness of the titanium wall was fixed to 1 cm, while the zirconium wall of the radiotoxic isotope container had a thickness of 0.5 cm.

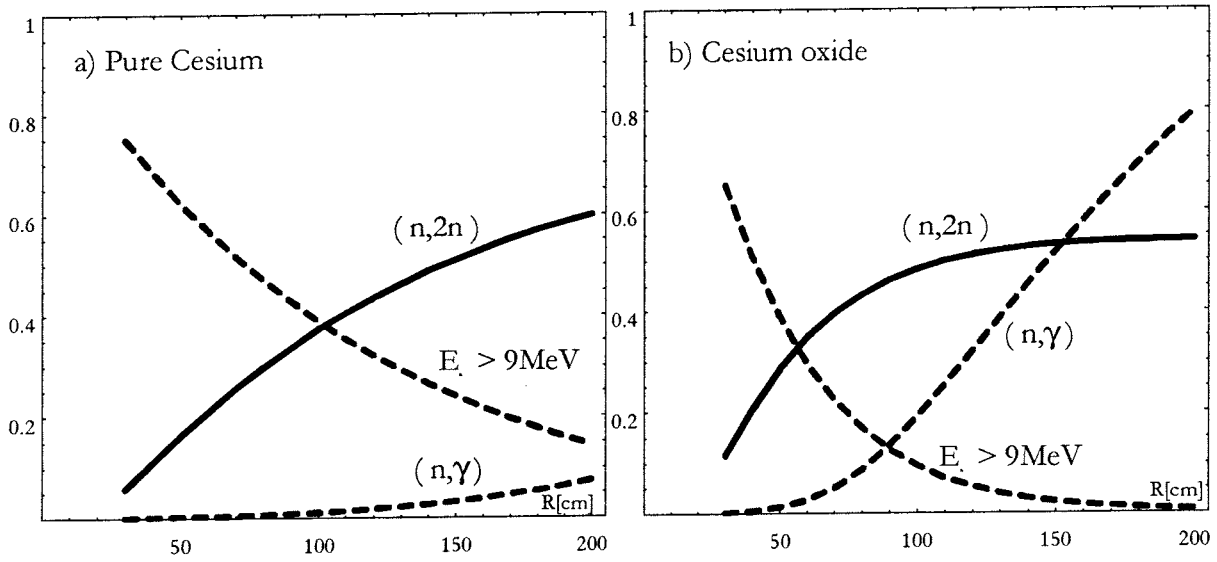

Fig. 3: The fraction of neutrons (relative to the number of source neutrons) inducing transmutation reactions in ^{137}Cs for a pure ^{137}Cs inventory (a) and a Cs_2O compund (b). Numbers are given as a function of transmutation chamber radius. Also shown is the fraction escaping the transmutation chamber with energy above the (n,2n) reaction threshold.

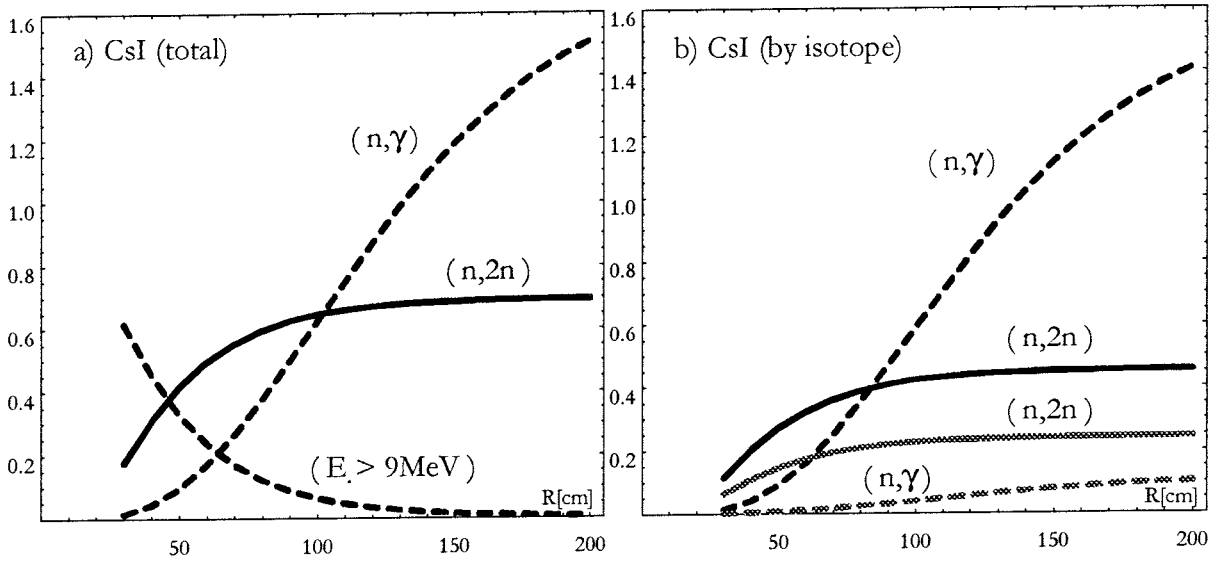

Fig 4: The fraction of neutrons (relative to the number of source neutrons) inducing transmutation reactions in ^{137}Cs and ^{129}I for a CsI salt inventory. In (a) total numbers are given, together with the fraction escaping with energies above the (n,2n) reaction threshold. In (b) figures are given for the isotopes separately, ^{137}Cs denoted with gray lines, ^{129}I with black.

Table I: Transmutation efficiencies, transmutation rates and the fraction of initial ^{137}Cs mass transmuted within one natural half-life as function of ^{137}Cs mass within a sphere of radius R containing Cs_2O salt. E_b = 4 GeV, I_d = 100 mA, $I_n = 5*10^{18}\ s^{-1}$.

R [cm]	30	40	50	60	70	100	150	200
m_{Cs} [tons]	0.3	0.8	1.6	2.8	4.4	13.2	45.0	107.1
η_{tr}	0.11	0.21	0.30	0.37	0.44	0.67	1.05	1.34
λ_{tr} [kg/year]	4.5	8.3	11.7	14.7	17.5	26.5	41.3	52.6
$2T_{1/2}\lambda_{tr}/m_{Cs}$	0.92	0.64	0.45	0.32	0.24	0.12	0.06	0.03